JOURNAL OF COMPUTATIONAL PHYSICS 92, 106–141 (1991)

A Family of Methods for the Solution of Lattice Models

LEI GONG-YAN

Department of Mathematics, Peking University, Peking, China 100871; and Department of Mathematics and Lawrence Berkeley Laboratory, University of California, Berkeley, California 94720

Received June 3, 1986; Revised November 21, 1989

We discuss a family of methods for evaluating the thermodynamic functions for a class of lattice models that includes the Ising model. It is shown that the usual transfer-matrix method can be considered as a member of the family. Some typical members of this family are also introduced. Furthermore, we are concerned with the acceleration of these methods. For this reason an extra linear extrapolation algorithm, which is based on the member of this family related to the transfer-matrix method, is presented. By this algorithm, not only can the bulk physical quantities be evaluated more precisely but also an approximation to the boundary thermodynamic quantities can be obtained. A new expression for the boundary free energy of the Ising model is derived. In addition, the convergence to the thermodynamic limit is proven for the scaling method presented by Chorin. Some numerical results for the bulk and boundary thermodynamic functions of the Ising model are included.

1. INTRODUCTION

In this paper there are two goals. The first is the development of a family of methods for exactly and rapidly evaluating the partition function and other thermodynamic quantities for a class of finite-lattice models that includes the Ising model. All methods in this family are closely related to the linkage algorithm [II, 8]. The other goal is the development of some extrapolation methods which accelerate the convergence of finite-volume data to their thermodynamic limits.

In [II, 8], several methods for reducing the amount of labor required for the evaluation of the thermodynamic functions for lattice models were presented. Among these methods the basic one is the linkage algorithm, which relates the partition function and the free energy of a union of blocks to the same quantities evaluated on the component blocks. This linkage algorithm leads to an exact and fast enumeration scheme that reduces drastically the labor required for evaluating the partition function of a finite lattice: for example, for L Ising spins in the plane, the number of terms to be evaluated is reduced from 2^L to $L2^{\sqrt{L}}$. On the other hand two methods which accelerate the rate at which quantities evaluated on a finite lattice converge to their thermodynamic limits were presented in [II, 8]. One was called the factored solution. Chorin showed that for Ising spins on a line the thermodynamic limit was reached immediately by the factored solution. For a

0021-9991/91 $3.00

two-dimensional Ising model the numerical results showed that this algorithm accelerates the convergence. The other method was "scaling," which further accelerates the convergence of the factored solution. In [II, 8] there was only a heuristic justification for the method and the numerical results provided were for only one lattice size, which was not sufficient to show the convergence to the thermodynamic limit.

The present paper is based on [II, 8]. First, it is demonstrated that from the linkage algorithm a family of methods can be derived and the usual transfer-matrix method can be related to this family. In addition, a very flexible and efficient linkage method called the one-spin-at-a-time process is introduced. We show, in particular, that the partition function of an $m \times n$ rectangle can be computed by the one-spin-at-a-time process in a time of order $2^m mn$, compared to a time of order $2^{2m}(m+n)$ for the usual transfer-matrix algorithm. This part of the paper can be considered as an extension or a further explanation for the linkage algorithm. Second, we discuss the further acceleration for the methods in our family. It is shown that in mathematics Chorin's factored solution is an extrapolation method, and that in physics it is equivalent to the elimination of boundary effects. Furthermore, an extra linear extrapolation algorithm, which is based on the factored solution, for the member of this family related to the transfer-matrix method, is presented. By this algorithm not only can the bulk physical quantities be evaluated more precisely, but also an approximation to the boundary quantities can be obtained at the same time. Along the line of the algorithm a new expression for the boundary free energy of the Ising model is derived. Third, some numerical results, which show that when the lattice size increases, the thermodynamic functions computed by the scaling and the extra linear extrapolation algorithm converge to their thermodynamic limits, are included. Then a brief review of the factored solution, the scaling method, and the extra linear extrapolation algorithm is given.

In order to accelerate the convergence of finite-lattice sequences to their bulk limits, various extrapolation methods have been considered [I, 1; I, 2]. In fact, the analysis of numerical finite-lattice data by finite-size scaling theory is essentially an extrapolation problem. In connexion with this theory, a computationally important development is the phenomenological renormalization presented by Nightinggale [II, 15–16]. In addition, some sequence-transformation methods have been used to extrapolate the bulk critical parameters from the data for finite lattices with periodic boundary conditions [I, 1; II, 12]. These sequence-transformation methods have yielded some accurate results. However, they are general methods which have been used widely in the numerical analysis field and, generally speaking, do not have an explicit physical explanation. In the present paper we discuss the extrapolation problems, but we consider only the finite lattices with free boundary conditions because these lattices are suitably computed by the linkage algorithm. Also, we do not start with finite-size scaling. Without consideration of all finite-size effects, our attention is focused on the effect due to the "dangling bonds" at the boundary [I, 7]. Our extrapolation process is equivalent to elimimating this boundary effect from bulk thermodynamic quantities computed for a finite system.

By our extrapolation method both the bulk and the boundary thermodynamic functions can be studied.

For simplicity, we concentrate on the two-dimensional Ising model with free edges. Both bulk and boundary thermodynamic functions are computed. Our numerical results are consistent with the theoretical predictions and comparable with the results in [I, 5; II, 10; II, 13–15]. The numerical results for boundary thermodynamic quantities are given here apparently for the first time. The two-dimensional Ising model is discussed as an illustration. All of these methods can be applied to more complicated lattice systems.

This paper is organized as follows. In Section 2 we briefly describe the Ising model and some relevant theoretical results. In Section 3, in a slightly more general way, we discuss the linkage algorithm and then introduce a family of methods derived from the linkage. In Section 4 we show that, in essence, the factored solution is an extrapolation. In Section 5 we give an extra linear extrapolation algorithm. Finally, in Section 6 we present the computational results.

In this paper we do not discuss the estimates of critical exponents. This work will be done in another article.

2. Problem and Notation

We briefly describe the ferromagnetic Ising model and some relevant theoretical results.

Consider an $m \times n$ rectangular lattice with sites (i, j), $1 \leqq i \leqq m$, $1 \leqq j \leqq n$, carrying spins μ_{ij}, $\mu_{ij} = \pm 1$. A set of possible values $\mu = \{\mu_{ij}\}$ is called a configuration. If a free boundary condition is imposed, the energy of a configuration, in appropriate units, is

$$E(\mu) = -\sum_{i=1}^{i=m-1} \sum_{j=1}^{j=n} \mu_{i,j}\mu_{i+1,j} - \sum_{i=1}^{i=m} \sum_{j=1}^{j=n-1} \mu_{i,j}\mu_{i,j+1}. \tag{2.1}$$

When we consider different boundary conditions, for example, if we suppose that the lattice is wrapped as a torus, which means that the periodic boundary conditions are imposed both on the rows and on the columns of the lattice, the summation limits in (2.1) should be modified properly.

For the finite lattice the partition function is defined as

$$Z_{m\times n} = \sum_{\{\mu\}} \exp(-\beta E(\mu)), \tag{2.2}$$

where $\beta = 1/T$ and T is the temperature. The free energy $\phi_{m\times n}$ per spin for the finite lattice is

$$\phi_{m\times n} = (m \times n)^{-1} \log Z_{m\times n}. \tag{2.3}$$

In the thermodynamic limit the bulk free energy per spin is

$$\phi = \lim_{m, n \to \infty} \phi_{m \times n}. \tag{2.4}$$

Incidentally, the value of ϕ does not depend on the shape of the finite volumes used in taking the limit, or on the boundary conditions (see [I, 4]). The bulk internal energy U is

$$U = -\frac{\partial \phi}{\partial \beta}, \tag{2.5}$$

and the bulk specific heat C is

$$C = \beta^2 \frac{\partial U}{\partial \beta}. \tag{2.6}$$

In the Ising model a critical point β_c, i.e., a non-analytic point of ϕ, is found, $\sinh(2\beta_c) = 1$, $\beta_c = 0.440685\ldots$. The singularities of various physical quantities are characterized by the corresponding critical exponents. The critical exponents of the Ising model are known. In particular, the bulk specific heat C diverges logarithmically at β_c; in standard notation, the corresponding critical exponents $\alpha = \alpha' = 0_{\log}$ (see [I, 6]).

For a finite lattice at the criticality the behaviours of thermodynamic quantities differ from those of their thermodynamic limits and depend on the finite-size geometry and boundary conditions, which are described by the finite-size-scaling theory [I, 1; II, 1–3; II, 6–7]. For example, Fisher and Ferdinand, [II, 10] have shown that for an $m \times n$ Ising lattice with periodic boundary conditions, the specific heat does not diverge at β_c; rather, it exhibits a marked anomaly, whose height increases with the lattice size. The position $T_{\max}$ of the peak can be regarded as a pseudo-critical temperature and

$$(T_{\max} - T_c)/T_c \sim 1/n, \qquad n \to \infty, \ m/n \text{ fixed}. \tag{2.7}$$

Besides $T_{\max}$, there exists another significant temperature, namely the rounding temperature T^*, at which the specific heat curve for the finite lattice departs significantly from the bulk one and

$$(T^* - T_c)/T_c \sim 1/n, \qquad n \to \infty, \ m/n \text{ fixed}. \tag{2.8}$$

The reader should refer to [I, 1; II, 9] for details.

In order to define the boundary thermodynamic quantities, following [I, 1; I, 7], we consider an infinitely long ferromagnetic Ising strip consisting of m Paralle layers with free boundary conditions. At the temperatures away from the criticality we have

$$\phi_m = \phi + 2m^{-1} f + o(m^{-1}), \qquad m \to \infty, \tag{2.9}$$

where ϕ_m is the free energy per spin of the strip, $\phi_m = \lim_{n\to\infty} \phi_{m\times n}$. ϕ, as before, is the thermodynamic limit, $m^{-1}f$ stands for the correction due to the boundary effect, and f is the free energy per unit boundary length (for this boundary each unit length corresponds to one statistical degree of freedom). In (2.9), the factor 2 before $m^{-1}f$ comes from the two boundaries, upper and lower (in some references, for example, [I, 7], this factor is omitted). From (2.9) the boundary free energy per unit length in the thermodynamic limit is defined as

$$f = 2^{-1} \lim_{m\to\infty} m(\phi_m - \phi) \tag{2.10}$$

(assuming that this limit exists; see [I, 7]). Then, the boundary internal energy is

$$e = -\frac{\partial f}{\partial \beta}. \tag{2.11}$$

The boundary specific heat is

$$c^{\mathrm{b}} = \beta^2 \frac{\partial e}{\partial \beta}. \tag{2.12}$$

It is clear that the equations similar to (2.10) which relate the boundary thermodynamic quantities with the corresponding bulk quantities hold for e and c^{b}.

Here, it should be pointed out that at the criticality Eq. (2.9) will break down and the behaviours of both bulk and boundary thermodynamic quantities are predicted by the finite-size-scaling theory [I, 1; I, 7]. Presumably, the rounding temperature T^* is in some sense the limit of validity of the simple decompositions of the thermodynamic quantities into the bulk terms plus size-dependent corrections [I, 1].

In the two-dimensional Ising model there is only one critical point; i.e., the singularities in the boundary thermodynamic quantities occur exactly at the same temperature as those in the bulk properties. It is known that in the thermodynamic limit e diverges logarithmically at β_{c} and superimposed on the logarithmic infinity, there is a discontinuity in e at β_{c}, i.e.,

$$\lim_{\delta\to 0_+} (e(\beta_{\mathrm{c}} + \delta) - e(\beta_{\mathrm{c}} - \delta)) = L. \tag{2.13}$$

In the situation of free edges $L = \frac{1}{2}$ (if the factor 2 is omitted in (2.9), $L = 1$). In physics this phenomenon can be explained by "latent heat." The boundary specific heat c^{b} has a singularity t^{-1} (here $t = T/T_{\mathrm{c}} - 1$), which means that c^{b} has opposite signs above and below T_{c}. The critical exponents of c^{b} are $\alpha_s = \alpha_s' = 1$ [I, 7].

Now the problems are how to evaluate the thermodynamic quantities for the finite Ising model and how to accelerate their convergences to the corresponding thermodynamic limits.

3. The Linkage Algorithm

The successive linkage algorithm presented by A. J. Chorin evaluates the partition function of a union of finite-lattice blocks in terms of the partition functions of the component blocks [II, 8]. In fact, by successive linkage a family of algorithms can be constructed. Any algorithm in this family is characterized by successive increases in the lattice size; however, each one has its own way to choose the component blocks. Here, we introduce these algorithms in a slightly generalized way.

First, we give the concept of the conditional (or parametrized) partition function. Consider a lattice A and let S be a subset of A. For a given $s \in \{-1, 1\}^S$, the partition function for A conditioned (or parametrized) on S is defined as

$$\Lambda_s^{A,S} \equiv \sum_{\sigma \in \{-1,1\}^{A \setminus S}} \exp(-\beta E(\sigma \oplus s)), \tag{3.1}$$

where $\sigma \oplus s$ denotes the spin configuration which equals σ on $A \setminus S$ and equals s on S, and $E(\sigma \oplus s)$ is given by (2.1). Note that if $s_1 \subset s_2$, we have

$$\Lambda_{s_1}^{A,S_1} = \sum_{s' \in \{-1,1\}^{S_2 \setminus S_1}} \Lambda_{s_1 \oplus s'}^{A,S_2}. \tag{3.2}$$

Especially, the partition function Z^A for a lattice A can be expressed as $\Lambda^{A,\phi}$, where ϕ is the empty set, or

$$Z^A = \sum_{s \in \{-1,1\}^S} \Lambda_s^{A,S} \tag{3.3}$$

for any $S \subset A$.

Next, we consider the linkage of two sets. Let A and B be disjoint finite subsets of a graph G. Let A_B (resp. B_A) be the set of sites in A (resp. B) which are nearest neighbours of one or more sites in B (resp. A). Let S (resp. T) be a subset of A (resp. B) which contains A_B (resp. B_A). Let R be a subset of $S \cup T$. Then, the identity

$$\Lambda_r^{A \cup B, R} = \sum_{\sigma \in \{-1,1\}^{(S \cup T) \setminus R}} \Lambda_{(\sigma \oplus r)|S}^{A,S} \Lambda_{(\sigma \oplus r)|T}^{B,T} \exp(-\beta E((\sigma \oplus r)|A_B; (\sigma \oplus r)|B_A)) \tag{3.4}$$

holds. Here $|$ denotes restriction of a spin configuration to a subset and

$$\begin{aligned} E(s; t) &\equiv \text{interaction energy between } s \text{ and } t \\ &\equiv E(s \oplus t) - E(s) - E(t). \end{aligned} \tag{3.5}$$

Equation (3.4) expresses the linkage of disjoint sets A and B to form a combined set $A \cup B$. In order to perform the linkage, it is necessary that the partition functions of A and B be parametrized by sets S and T which contain at least the

relevant boundary points A_B and B_A, respectively; otherwise it would be impossible to compute the interaction energy between A and B. However, the sets S and T may optionally be larger than this; this can be useful in order to make possible subsequent linkage steps (as is explained below). Finally, the resulting partition function for $A \cup B$ may be parametrized by any desired subset $R \subset S \cup T$; the spins in $(S \cup T) \backslash R$ are summed over. Usually the graph G will be the simple-(hyper) cubic lattice Z^d with nearest-neighbor linkages, but the more general formalism allows treatment of other lattices, non-nearest- neighbor interactions, periodic and anti-periodic boundary conditions, etc.

The computational labor required for this linkage step is of order $2^{|(S \cup T)|}$ times the labor involved in the computation of $\exp(-\beta E(..., ...))$. The latter labor is $O(1)$ if it is dominated by the computation of the exponential, or $O(\#(A, B))$ if it is dominated by the computation of the interaction energy—here $\#(A, B)$ is the number of bonds of G which link A with B.

Now we introduce the successive linkage algorithm. In order to evaluate the partition function of a large lattice, we can start with a small block, then repeatedly apply the two-set linkage step explained above until the required lattice has been formed. It is obvious that the initial block A and the successive linked blocks B's can be chosen in many different ways: thus, from these different choices a family of methods can be formed. In some cases the linked blocks B's in any step have the same geometry as the initial block. One such block will be called a basic block. The family of successive linkage algorithms includes special significant cases, some of which are listed below.

(a) *The Transfer-Matrix Method*

The usual transfer-matrix method can be carried out by a successive linkage algorithm. Consider an $m \times n$ Ising model with free boundary conditions. The partition function $Z_{m \times n}$ is given by (2.2). Denote a column configuration by σ_j, i.e.,

$$\sigma_j = (\mu_{1,j}, \mu_{2,j}, ..., \mu_{m,j});$$

then, there is a total of 2^m possible configurations for each σ. We can associate each configuration with an integer between 1 and 2^m according to the rule

$$\sigma = \sigma(i), \qquad i \to 1 + \sum_{k=1}^{m} \max(0, \mu_k) \cdot 2^{k-1}. \tag{3.6}$$

If we define

$$V_1(\sigma_j) = -\sum_{i=1}^{m-1} \mu_{i,j} \mu_{i+1,j},$$

$$V_2(\sigma_j, \sigma_{j+1}) = -\sum_{i=1}^{m} \mu_{i,j} \mu_{i,j+1}$$

then, the partition function $z_{m\times n}$ can be written as

$$z_{m\times n}=(\alpha, L^{n-1}\alpha), \tag{3.7}$$

where $\alpha=(\alpha_1, \alpha_2, ..., \alpha_{2^m})^{\mathrm{T}}$ is a vector defined by $\alpha_i=\exp(-\beta/2\, V_1(\sigma(i)))$, $i=1, 2, ..., 2^m$, and L is a $2^m\times 2^m$ matrix whose (σ, σ') component is given by

$$L(\sigma, \sigma')=\exp\left(-\frac{\beta}{2}V_1(\sigma)\right)\exp(-\beta V_2(\sigma, \sigma'))\exp\left(-\frac{\beta}{2}V_1(\sigma')\right). \tag{3.8}$$

Usually, matrix L is called the transfer matrix. Note that matrix L is symmetric and its elements are all positive; therefore, it has complete eigenvectors and its maximum eigenvalue λ_1 is strictly nondegenerate. Thus, from (3.7) it is easy to see that for an $m\times\infty$ Ising strip the free energy per spin is given by

$$\begin{aligned}\phi_{m\times\infty}&=\lim_{n\to\infty}\phi_{m\times n}=\lim_{n\to\infty}(m\times n)^{-1}\log z_{m\times n}\\&=m^{-1}\log\lambda_1.\end{aligned} \tag{3.9}$$

The conventional transfer-matrix method first forms the $2^m\times 2^m$ matrix L, then, by a certain numerical method, calculates the dominant eigenvalue λ_1 of L. Thus, an approximation to $\phi_{m\times\infty}$ is obtained.

However, from (3.9) we know that for sufficiently large n, $\phi_{m\times n}$ can also be considered as an approximation to $\phi_{m\times\infty}$. By a successive linkage algorithm for any $m\times n$ rectangular lattice the thermodynamic quantities can be calculated; that is to say, in essence, the transfer-matrix method can be carried out by a successive linkage algorithm. For this purpose it is only necessary that in Eq. (3.4) we take the set A to be an $m\times l$ rectangle parametrized by $S=$ its rightmost column, the set B to be an $m\times 1$ rectangle (vertical column) parametrized by $T=B$, and the set R to be T. Then $A\cup B$ is an $m\times(l+1)$ rectangle, parametrized by $R=$ its rightmost column, so that the procedure can continue repeatedly; thus, for any large n, $Z_{m\times n}$ can be computed, and therefore, the approximation to $\phi_{m\times\infty}$ with any accuracy can be obtained. For simplicity, we can first take $l=1$, i.e., $A=B=$ an $m\times 1$ rectangle parametrized by itself. This vertical column containing m spins is a basic block.

By the above-mentioned method, in order to compute the partition function $Z_{m\times n}$ for an $m\times n$ rectangle the computational labor is roughly of order $2^{2m}n$. There are 2^{2m} possible configurations of spins in the two columns to be linked at each step and this linkage step must be repeated n times. For each linkage step, it is necessary to compute the interactive energy $E(s, t)$ for any possible configuration of s and t; however, it is noted that these interactive energys do not vary with n, so, we can set up a table of $E(s, t)$ for all possible pairs of s and t beforehand. The computational labor for the pre-processing (setting up the table) is of order $2^{2m}m$. Thus, the local labor is of order $2^{2m}(m+n)$.

It is also possible to consider the linkage method in which at each stage the number of columns of the rectangle currently being processed is doubled. We begin from

an $m \times 2$ rectangle and in each step we need to parametrize both vertical edges of the present block. In order to compute an $m \times n$ lattice by this method, the labor is roughly of order $2^{4m} \log_2 n$ (the procedure should be repeated $\log_2 n$ times, at each step there are 2^{2m} configurations, and for each configuration the labor is roughly of order 2^{2m}).

In principle, the above successive linkage algorithm can be used instead of the usual transfer-matrix method. However, it is difficult to compare their computational labors because when an m is given, we do not know, for the above-mentioned method, how large an n is needed. But, there is no need to be concerned about this, as in Section 4 it is demonstrated that by a slightly different successive linkage algorithm, followed by a simple extrapolation, the transfer-matrix method can be carried out thoroughly, and in comparison with the conventional transfer-matrix method, the computational labor is drastically reduced.

It should be pointed out that the above-mentional successive linkage algorithm can be applied to rectangles with periodic boundary conditions in the vertical (m) direction. Note also that the successive linkage algorithm can be generalized to the three-dimensional case.

(b) *Chorin's Method for Linkage of Four Blocks*

In [II, 8], A. J. Chorin has presented a method for linkage of four blocks. This method relates closely to an extrapolation algorithm called the particular factored solution, which is discussed in the next section.

Consider an $m \times n$ Ising lattice, which we take as a basic block. For the basic block the partition function is parametrized on two adjacent edges. Note that for any pair of adjacent edges, because of the symmetry, the sets of conditional partition functions are the same. From (3.3), for the basic block the partition function Z^{B} can be expressed as

$$Z^{\mathrm{B}} = \sum_{s_{\mathrm{b}} \oplus s_{\mathrm{r}}} \Lambda^{B,\, S_{\mathrm{b}} \cup S_{\mathrm{r}}}_{s_{\mathrm{b}} \oplus s_{\mathrm{r}}}, \tag{3.10}$$

where S_{b} stands for the bottom edge and S_{r} for the right edge. From $\Lambda^{B,\, S_{\mathrm{b}} \cup S_{\mathrm{r}}}_{s_{\mathrm{b}} \oplus s_{\mathrm{r}}}$, as shown in Fig. 1, a $2m \times 2m$ lattice containing four basic blocks can be constructed. The partition function of two blocks, parametrized on $S_{\mathrm{b}} \cup S_2$, is

$$Z^{2B} = \sum_{s_{\mathrm{b}} \oplus s_2} \Lambda^{2B,\, S_{\mathrm{b}} \cup S_2}_{s_{\mathrm{b}} \oplus s_2}, \tag{3.11}$$

where

$$\Lambda^{2B,\, S_{\mathrm{b}} \cup S_2}_{s_{\mathrm{b}} \oplus s_2} = \sum_{s_{\mathrm{r}} \oplus s_1} \Lambda^{B,\, S_{\mathrm{b}} \cup S_{\mathrm{r}}}_{s_{\mathrm{b}} \oplus s_{\mathrm{r}}} \Lambda^{B,\, S_1 \cup S_2}_{s_1 \oplus s_2} \exp(-\beta E(s_{\mathrm{r}}, s_1)). \tag{3.12}$$

In (3.12), the symbols are simplified in comparison with those in (3.4). However for the special case, the meaning is still clear.

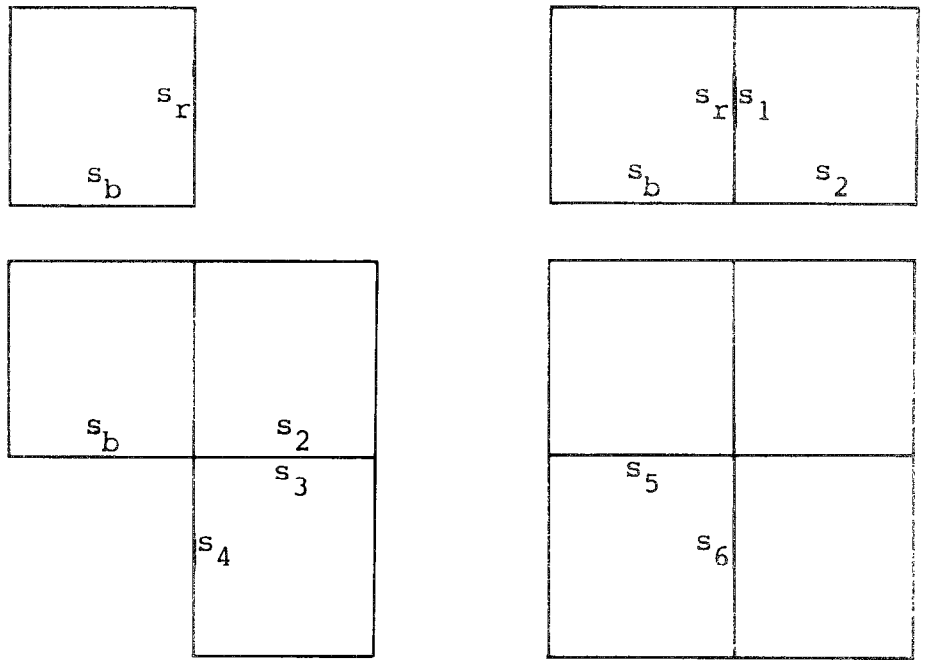

FIG. 1. Chorin's method for linkage of four blocks.

In the next step, we have

$$Z^{3B} = \sum_{s_b \oplus s_4} \Lambda^{3B,\, S_b \cup S_4}_{s_b \oplus s_4}, \tag{3.13}$$

where

$$\Lambda^{3B,\, S_b \cup S_4}_{s_b \oplus s_4} = \sum_{s_2 \oplus s_3} \Lambda^{2B\, S_b \cup S_2}_{s_b \oplus s_2} \Lambda^{B.\, S_3 \cup S_4}_{s_3 \oplus s_4} \exp(-\beta E(s_2, s_3))$$

and finally $Z_{2m \times 2m}$ is

$$Z_{2m \times 2m} = Z^{4B} = \sum_{s_5 \oplus s_6} \sum_{s_b \oplus s_4} \Lambda^{3B,\, S_b \cup S_4}_{s_b \oplus s_4} \Lambda^{B,\, S_5 \cup S_6}_{s_5 \oplus s_6} \exp(-E(s_b \oplus s_4, s_5 \oplus s_6)). \tag{3.14}$$

The cost of computing $Z_{m \times m}$ parametrized on two adjacent edges is of order 2^{m^2}. This parametrized partition function can then be stored and the three linkage steps require an amount of labor of order 2^{4m} each, which is negligible compared to 2^{m^2} if m is large; therefore the cost of computing $Z_{2m \times 2m}$ by the method just described is of order 2^{m^2}. The cost of evaluating $Z_{2m \times 2m}$ directly, without linkage, is of order 2^{4m^2}. The linkage algorithm reduces the amount of labor by a factor of $\sim 2^{3m^2}$. This algorithm has another advantage: by a simple method which is explained in Section 4, its results can be extrapolated easily.

However, the algorithm just described also has a defect: the input is the partition function of an $m \times m$ block parametrized by the spins on its two adjacent edges, but the output is the partition function of a $2m \times 2m$ block parametrized by nothing (or parametrized by some of the internal spins $s_b \oplus s_r \oplus s_1 \oplus s_2 \oplus s_3 \oplus s_4 \oplus s_5 \oplus s_6$), so the procedure cannot be repeated to construct a still large block. In principle, we can overcome this disadvantage, by designing a method for repeated linkage of square blocks. Let the input be the partition function of an $m \times m$ block, parametrized by all its boundary spins. Then, successive linkage as shown in Fig. 1 yields the partition function of a $2m \times 2m$ block, again parametrized by all its boundary spins, and so the process can be repeated to form a $4m \times 4m$ block, an $8m \times 8m$ block, etc. Then it is easy to see that the labor for computing $Z_{2^k m \times 2^k m}$ (m fixed, k large) is dominated by the *last* linkage step (i.e., $2^{k-1}m \to 2^k m$), and is of order $2^{4 \cdot 2^k m}$. That is, the labor for computing $Z_{n \times n}$ (at least for n equal to a power of 2 times a small integer) is of order 2^{4n}, as compared to 2^{n^2} for a direct evaluation. However, this algorithm has a severe difficulty: it demands too much storage space. The partition function parametrized by all boundary spins for a 4×4 block has 2^{12} terms, and for an 8×8 block the number increases rapidly to 2^{28}, and each term should be stored separately. For this reason, it is difficult to perform this algorithm on the present computers.

Obviously, there are also some methods intermediate between the method for linkage of four blocks and the above-mentioned ideal method. They have the same disadvantage of principles as method (b), but they might satisfy some special need. However, we do not dwell on them. Instead of describing particular algorithms, here we introduce the one-spin-at-a-time process, which is a simple and efficient algorithm. Moreover, many other successive linkage algorithms, e.g., methods (a) and (b), can be carried out by this process.

(c) *One-Spin-at-a-Time Process*

In this algorithm we use one spin as the basic block; i.e., we start with one spin and during the successive linkage process in each step only one spin is added. As an example, we show how the partition function of an $m \times n$ lattice can be computed by this process. This process was first used by A. J. Chorin.

First, we link two spins; $\mu_{1,1}$ and $\mu_{2,1}$, as shown in Fig. 2a; they are arranged in a column. For the two spins there are four configurations: $(-1, -1)$, $(-1, 1)$, $(1, -1)$, $(1, 1)$. The corresponding conditional partition functions are $\Lambda_{-1,-1} = e^{\beta}$, $\Lambda_{-1,1} = e^{-\beta}$, $\Lambda_{1,-1} = e^{-\beta}$, and $\Lambda_{1,1} = e^{\beta}$, respectively, which will be stored in an array A containing four elements and the corresponding subscripts are calculated according to rule (3.6). Thus, if the subscript is odd, it means that this conditional partition function corresponds to a configuration, for which the last spin is down; otherwise, the last spin is up. Now we add a spin $\mu_{3,1}$ to the block formed by $\mu_{1,1}$ and $\mu_{2,1}$ on the bottom and consider the partition function for the augmented block. The partition function for the three-spin block $(\mu_{1,1}, \mu_{2,1}, \mu_{3,1})$ conditioned on itself has 2^3 terms, and each term will be stored in an element of an array B and calculated as follows:

When the added spin $\mu_{3,1}$ is up, i.e., $\mu_{3,1}=1$,

$$B(2i)=A(i)*e^{-\beta}, \qquad i=1,3,$$
$$B(2i)=A(i)*e^{\beta}, \qquad i=2,4.$$

When the added spin $\mu_{3,1}$ is down, i.e., $\mu_{3,1}=-1$,

$$B(2i-1)=A(i)*e^{\beta}, \qquad i=1,3,$$
$$B(2i-1)=A(i)*e^{-\beta}, \qquad i=2,4.$$

Note that for array B, the subscripts still obey rule (3.6). We continue the process until an $m\times 1$ column has been formed. For the column containing m spins, the

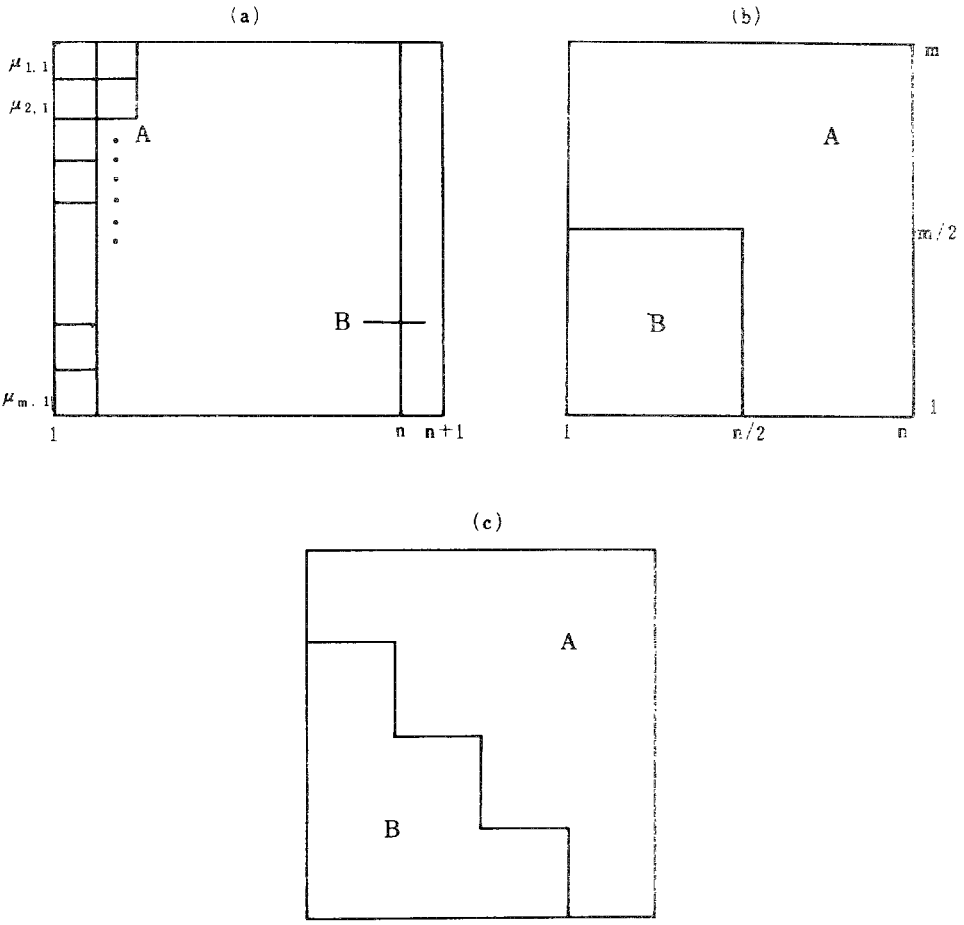

FIG. 2. Some possible choices of blocks A and B.

partition function conditioned on itself has 2^m terms, which are stored in an array containing 2^m elements. For simplicity, we continue to denote the array by character A. Because rule (3.6) is still correct, we can determine from the subscript of any element of A the configuration which corresponds to the conditional partition function stored in this element.

Now suppose that an $m \times (l-1)$ lattice has been constructed, and that its partition function is parametrized by its rightmost column and stored in an array A containing 2^m elements according to rule (3.6). We consider how an $m \times l$ lattice can be calculated by continuously using the one-spin-at-a-time process.

First, spin $\mu_{1,l}$ is added. Note that for the $m \times (l-1)$ lattice already formed, spin $\mu_{1,l}$ interacts only with spin $\mu_{1,l-1}$, and for each $A(i)$, the value of $\mu_{1,l-1}$ can be determined from the corresponding subscript i. Thus, from the linkage of $\mu_{1,l}$ for each $A(i)$ we obtain two terms: one is $A(i)\, e^{\beta\mu_{1,l-1}}$, another is $A(i)\, e^{-\beta\mu_{1,l-1}}$, and they correspond to $\mu_{1,l}=1$ and $\mu_{1,l}=-1$, respectively. So, there is a total of 2^{m+1} terms, which give the partition function of the $m \times (l-1)$ lattice with spin $\mu_{1,l}$ added, parametrized by the $(l-1)$st column and $\mu_{1,l}$. Note that after the linkage of $\mu_{1,l}$, the value taken by spin $\mu_{1,l-1}$ is useless, so the partition function after linkage of $\mu_{1,l}$ can be parametrized only by spins $\mu_{1,l}, \mu_{2,l-1}, \mu_{3,l-1}, \ldots, \mu_{m,l-1}$. That is to say, the 2^{m+1} terms just obtained can be reduced to 2^m terms, and they can still be stored in the original array A. However, at this moment, the subscripts of A correspond to the configurations of set $(\mu_{1,l}, \mu_{2,l-1}, \ldots, \mu_{m,l-1})$.

Next, we adjoint spin $\mu_{2,1}$ to the lattice part just formed. The procedure is very similar to that described above for the linkage of spin $\mu_{1,l}$. The only difference is that in order to calculate the new conditional partition functions, for each $A(i)$, we need to abstract the information about the values taken by spins $\mu_{1,l}$ and $\mu_{2,l-1}$ from subscript i, because both $\mu_{1,l}$ and $\mu_{2,l-1}$ will interact with $\mu_{2,l}$. Then, for each $A(i)$, we obtain two terms; $A(i)\, e^{\beta(\mu_{1,l}+\mu_{2,l-1})}$ and $A(i)\, e^{-\beta(\mu_{1,l}+\mu_{2,l-1})}$, which correspond to $\mu_{2,l}=1$ and $\mu_{2,l}=-1$, respectively. There is also a total of 2^{m+1} terms, which, similarly, can be reduced to 2^m terms, giving the partition function for the $m \times (l-1)$ lattice plus spins $\mu_{1,l}$ and $\mu_{2,l}$ parametrized on set $(\mu_{1,l}, \mu_{2,l}, \mu_{3,l-1}, \ldots, \mu_{m,l-1})$. Obviously, this procedure can be repeated until the whole $m \times n$ lattice has been formed. Then, the partition function for the whole $m \times n$ lattice, parametrized by its last column, is obtained.

In the above the one-spin-at-a-time process is merely sketched. Here some additional explanations should be given:

First, note that Eq. (3.4) can be differentiated with respect to β, so the one-spin-at-a-time process yields not only the free energy for an $m \times n$ lattice but also the

$e^{-\beta}$) can be done once and for all. This will reduce the computational labor significantly.

Third, the one-spin-at-a-time process is very flexible and can be used in many different cases. For example, the usual transfer-matrix method and Chorin's method for linkage of four blocks can both be carried out by this process, and obviously,

this algorithm can also be generalized to a three-dimensional model. However, this algorithm is not suitable for models with periodic boundary condition. Thus, for this algorithm it is necessary to consider extrapolation methods that eliminate boundary effects.

Finally, we estimate the computational labor required by the one-spin-at-a-time process. In order to calculate the conditional partition functions for the first column of an $m \times n$ lattice, the computational labor must be of order 2^m. Then, if we take the labor required by a one-spin linkage as a unit, the total computational labor will be of order $2^m mn$. *Thus, if we use the one-spin-at-a-time process to perform the usual transfer-matrix method, it will be better than algorithm (a).*

More generally, consider an arbitrary finite graph G with N vertices, and suppose that we wish to compute the partition function of the Ising model of G. Choose an ordering of the vertices, say $x_1, x_2, ..., x_N$. For each $j\,(1 \leqq j \leqq N-1)$, let M_j be the number of vertices $x_1, x_2, ..., x_j$ that are adjacent to one or more of the vertices $x_{j+1}, x_{j+2}, ..., x_N$, and let E_j be the number of edges connecting $x_1, x_2, ..., x_j$ to x_{j+1}. Then the computational labor for the one-spin-at-a-time process is of order $\sum_{j=1}^{N-1} 2^{M_j} E_j$, and the storage requirement is 2^M, where $M \equiv \max_{1 \leqq j \leqq N-1} M_j$. Note the importance of finding a "good" ordening of the vertices, i.e., one which minimize M (similar problems arise in sparse Gaussian elimination).

4. The Factored Solution—An Extrapolation Method

In [II, 8], Chorin has shown that the successive linkage of blocks results in an approximate factorization of the partition function of a lattice into terms associated with small blocks far from the unconnected edge. On this basis he has proposed an approximate factorization algorithm which accelerates the convergence of the quantities computed on a finite lattice to their thermodynamic limits. In this section we introduce this algorithm and demonstrate that this algorithm, i.e., the factored solution, is essentially an extrapolation method.

Consider a successive linkage process, in which an $m \times m$ lattice B is taken as a basic block. Suppose that a lattice A consisting of l basic blocks has already been formed and parametrized in a proper manner. In order to construct a still larger block, we continue in the next step to adjoin a basic block B to A, and according to Eqs. (3.4) and (3.3), the partition function $Z^{A \cup B}$ can be computed. If we define

$$\tilde{Z}_{l+1}\,(=\tilde{Z}_{B;A}) \equiv Z^{A \cup B}/Z^A, \tag{4.1}$$

then, $\tilde{Z}_{l+1}$ can be considered as the contribution of the newly connected $(l+1)$st block to the partition function $Z^{A \cup B}$, and Eq. (4.1) gives a factorization of $Z^{A \cup B}$. If the factors $\tilde{Z}_l\,(l = 1, 2, ...)$ obtained in a successive linkage process converge to a limit $\tilde{Z}_{m \times m}$ (for the one-dimensional Ising model, the existence of a similar limit is rigorously proved; for the two-dimensional case, generally speaking, it is an assumption), then,

$$\lim_{l\to\infty}\frac{1}{lm^2}\log Z^l=\lim_{l\to\infty}\frac{1}{lm^2}\sum_{k=1}^{l}\log\tilde{Z}_k$$

$$=\frac{1}{m^2}\log\tilde{Z}_{m\times m}, \tag{4.2}$$

where Z^l stands for the partition function of a lattice consisting of l basic blocks. Equation (4.2) shows that $(1/m^2)\log\tilde{Z}_{m\times m}$ is the free energy per spin in the thermodynamic limit. Note that Eqs. (4.2), (4.1), and (3.4) can be differentiated with respect to β and yield successive approximations $U_{m\times m}\to U$, $C_{m\times m}\to C$. Hereafter, for any sets A and B, the general operation expressed by (4.1) is called a factored operation.

In practice, it is impossible to obtain the limit factor $\tilde{Z}_{m\times m}$. An alternative approach is to perform the factored operation only once; i.e., we start with a lattice A chosen properly and then adjoin to it another B. Thus, according to (4.1), $\tilde{Z}_{B;A}$ is calculated and used as an approximation to $\tilde{Z}_{m\times m}$ in (4.2).

Next, for algorithms (a) and (b), explained in Section 3, we demonstrate how the factorization approximations can be carried out.

In the preceding section, it was shown that for an $m\times n$ Ising model with free boundary conditions, the partition function is

$$Z_{m\times n}=(\alpha, L^{n-1}\alpha), \tag{4.3}$$

where α is a vector and L is a matrix, both of which are well-defined. Equation (4.3) can be calculated by a successive linkage algorithm, in which an $m\times 1$ column is taken as a basic block, and in essence, this is the transfer-matrix method. From (4.3) it is easy to see that adjoining a column is equivalent to raising L by one power. Now consider the factorization approximation, and in (4.1), let $Z^{A\cup B}=Z_{m\times(n+1)}$ and $Z^A=Z_{m\times n}$, thus, from (4.2), the free energy per spin for an $m\times\infty$ Ising strip can be approximated by

$$\phi_{m,n+1}=\frac{1}{m}\log\frac{(\alpha, L^n\alpha)}{(\alpha, L^{n-1}\alpha)}=\frac{1}{m}\left(\log\lambda_1+O\left(\left(\frac{\lambda_2}{\lambda_1}\right)^{n-1}\right)\right), \tag{4.4}$$

where λ_1 is the largest eigenvalue of the $2^m\times 2^m$ matrix L. For fixed m and sufficiently large n, $\phi_{m,n}$ is a good approximation to $m^{-1}\log\lambda_1$ and has an error $O((\lambda_2/\lambda_1)^n)$. Thus, the factorization approximation (4.4) allows an easy extrapolation from an $m\times n$ lattice to an $m\times\infty$ lattice. The more important thing is that we know the factored operation expressed by (4.4) is equivalent to computing the maximum eigenvalue λ_1 of the transfer matrix L by the power method with n iterations. Thus, the usual transfer-matrix method can be carried out thoroughly by a successive linkage algorithm followed by an extrapolation.

From now on the method given by (4.4) will be called the *factored solution by*

column. We note that the accuracy obtained by this method is restricted by m. Visually, the reason for this is that it is an extrapolation along only one direction, i.e., the direction along which parameter n increases. In [II, 8], Chorin proposed another factorization algorithm based on the method for linkage of four blocks, which can be considered as an extrapolation along m and n in two directions.

For the method for linkage of four blocks, as explained in Section 3, an $m \times m$ Ising lattice is taken as a basic block. According to formulas (3.13) and (3.14), the partition functions Z^{3B} and Z^{4B} can be computed. In order to consider the factored approximation, in (4.1), let $Z^{A \cup B} = Z^{4B}$ $(= Z_{2m \times 2m})$, $Z^{A} = Z^{3B}$, and

$$\tilde{Z}_{m \times m} \cong Z^{4B}/Z^{3B}; \tag{4.5}$$

thus, a factored solution is obtained. For convenience, hereafter, this solution is called the *particular factored solution.* Numerical tests (see Section 6) have shown that the particular factored solution accelerates the convergence to the thermo dynamic limit, and it gives more accurate results than the factored solution by column and many other possible factored approximations which correspond to various different choices of sets A and B in the general formula (4.1). Now we explain heuristically the physical mechanism which we believe underlines this faster convergence.

It is well known that phase transitions in statistical mechanical calculations arise only in the thermodynamic limit. The thermodynamic limit requires that the linear dimension of a model system approach infinity. However, in any pratical computation only a finite lattice can be considered. An important part of the finite-size effect is due to the "dangling bonds" on the boundary [I, 1; I, 3; I, 6]. For the two-dimensional Ising model an inner spin has four adjacent spins. A pair of adjacent spins are interrelated through a bond and interact with each other. However, for free boundary conditions, the spins located on the boundary sites have no interaction with the outside, and thus the contribution of a boundary spin to the thermodynamic quantities differs from that of an inner spin. Since, in general, a unit boundary length corresponds to a dangling bond, this effect is proportional to the boundary length for the whole lattice system. More precisely, for a finite two-dimensional Ising lattice containing N sites and having boundary lenght L, from thermodynamics we can expect that [I, 1]

$$N\phi_N = N\phi + Lf + o(L), \tag{4.6}$$

where ϕ_N is the free energy per spin computed from the finite lattice, ϕ is the bulk thermodynamic limit, and f stands for the correction per unit boundary length due to the "dangling bonds." Now we inspect the particular factored solution from the point of view of boundary effects. It is found that although the rectangular lattice $A \cup B$ and the sub-lattice A in Fig. 2b contain different numbers of spins, they have the same boundary length. From (4.6) it is clear that $\log Z^{A \cup B}$ and $\log Z^{A}$ contain

the same boundary correction terms; that is to say, they contain almost the same boundary effect as that induced by the "dangling bonds." Therefore, when the thermodynamic limit.

From the above discussion it is plausible that the particular factored solution is better than the factored solution by column. For the factored solution by column, as shown in Fig. 2a, the lattice $A \cup B$ is an $m \times (n+1)$ rectangle and the sub-lattice A is an $m \times n$ rectangle. They have different boundary lengths. After the factored operation some boundary effects induced by the "dangling bonds" are still included in the numerical results. Thus, the particular factored solution is likely to be more accurate. It should be pointed out that for the factored solution by column, if periodic boundary conditions in the vertical direction are used, the boundary effects can also almost be cancelled. However, we would rather use the free boundary conditions than the periodic ones. The reason is that for free boundary conditions, the computation can be performed by the one-spin-at-a-time process, which is more efficient. In addition, it is shown in the next section that by a simple extra linear extrapolation, from the factored solution by column with free boundary conditions, not only can the bulk thermodynamic quantities be evaluated more precisely but also the approximations to the boundary thermodynamic quantities can be obtained at the same time.

In order to let sub-lattice A have the same boundary length as lattice $A \cup B$, lattice A can be chosen in many different ways. One such choice is shown in Fig. 2c, for which lattice A has a more complex shape. From (4.5), this choice corresponds to a factored method. For simplicity, hereafter we call it the *generalized factored solution*. Now we argue heuristically that the particular factored solution is likely to be better than the generalized one. In this discussion we are concerned with the spin effects which are located on corners. For the two-dimensional ferromagnetic Ising model in various wedge geometries the corner spin magnetization has been investigated by Barber *et al.* in [II, 4], but up to now the corner spin thermodynamic effect has not been clear, so we can discuss this question only qualitatively. However, the following discussion appears to be reasonable and the numerical calculations displayed in Table II and III support our conclusion. The reader should refer to [I, 1; I, 3; I, 7; II, 4] for related discussions.

Let us first analyze the boundary effect induced by "dangling bonds" more carefully. For an $m \times n$ lattice the boundary length is $2(m+n)$ and there are $2(m+n)-4$ spins located on the boundary. The boundary length is not equal to the boundary spin number because there are four convex corners. If the lattice were larger (e.g., $(m+1) \times (n+1)$), then the $2(m+n)-4$ spins which are currently on the boundary would interact with $2(m+n)$ spins surrounding them on the outside; therefore, we can consider that the boundary effect is equal to the interactions between the $2(m+n)-4$ boundary spins and the $2(m+n)$ imaged spins. A spin located on a convex corner has two dangling bonds and a general boundary spin has only one; thus, they have different contributions to the boundary effects. By this

consideration, for an $m \times n$ lattice with free boundary conditions, instead of Eq. (4.6), we conjecture that the expression

$$N\phi_N = N\phi + Lf + 4C_1 + o(L^{-1}), \qquad L \to \infty \tag{4.7}$$

should be correct. Here $N = m \times n$, $L = 2(m+n)$; ϕ_N, ϕ, f have the same meanings as in (4.6); and C_1 represents the correction due to one convex corner. The last term, $o(L^{-1})$, represents all the other finite-size effects. This seems reasonable because, after the "dangling bonds" effect has been separated from the others, the remaining finite-size effect can be considered as approximately the effect for a lattice with periodic boundary conditions, which is exponentially decreasing. For the sub-lattice A shown in Fig. 2b, the boundary spin number reduces to $2(m+n)-5$, because there are five convex corners. On the other hand, the spin number which surrounds this sub-lattice A is $2(m+n)-1$. This number is one less than the boundary length. The reason is similar: there is also a concave corner in A. The two boundary spins which form the concave corner would interact with only one imaged spin outside A; thus, the effects of these spins also differ from the effect of the general boundary spins. For the sub-lattice A the boundary effect due to the "dangling bonds" can be considered as the interaction between $2(m+n)-5$ boundary spins and $2(m+n)-1$ imaged spins. By a consideration similar to (4.7), for this sub-lattice we have

$$N_a\phi_{N_a} = N_a\phi + Lf + 5C_1 + C_2 + o(L^{-1}), \tag{4.8}$$

where, N_a is the number of spins contained in A, and C_2 represents the correction due to a concave corner. Further, we consider a general sub-lattice A, as shown in Fig. 2c, which still has the boundary length L, but l ($l \geqq 5$) convex corners (in the example shown in Fig. 2c, $l = 7$). In company with the l convex corners there must be $l-4$ concave corners. Thus for a general A, the boundary effect can be considered as the interactions between $2(m+n)-l$ boundary spins and $2(m+n)-(l-4)$ imaged spins. Instead of (4.8), generally we have

$$N_a\phi_{N_a} = N_a\phi + Lf + lC_1 + (l-4)\,C_2 + o(L_{-1}). \tag{4.9}$$

From (4.7) and (4.8) we know that the boundary effects due to the "dangling bonds" for the whole lattice and the sub-lattice A in Fig. 2b are not exactly the same; the difference between them is approximately $C_1 + C_2$, However, for a general sub-lattice A with l convex corners, the difference is $(l-4)(C_1+C_2)$. It is plausible that the larger the number l is, the more different the boundary effects between the $m \times n$ lattice and the sub-lattice A are. Consequently, after the factored operation more boundary effects will remain in $\log Z_B$. It affects the accuracy strongly.

From the above discussion we know that the particular factored solution is better than any general factored one, because in Fig. 2b, $l = 5$, it is the possible minimum value. Thus, for the particular factored solution the boundary effects due to the "dangling bonds" are almost cancelled.

Of course, in order to have $l=5$, it is not necessary for B to be exactly half the width of $A \cup B$. There are still some possible choices. However, numerical tests indicate that only for those B's whose widths are slightly less than half the width of $A \cup B$ are the results comparable with the particular factored solution. And for a 4×4 lattice the particular factored solution gives the best result. Therefore, we prefer the particular factored solution over the others.

5. An Extra Linear Extrapolation Algorithm

In the preceding section we showed that in essence the factored approximation is an extrapolation method. Especially, the particular factored solution and the factored solution by column were discussed. In this section we consider their further accelerations.

In [II, 8] a further acceleration method, which is based on the particular factored solution and is called the scaling, was presented. The basic idea is as follows: imagine a "spin bath" infinitely extending to the top and the right of a $2m \times 2m$ lattice. The spin bath imposes different weights on the configurations formed by the spins located on the top and the right boundary of the finite lattice. The method is an iterative one. It starts with a guess of the weights, which can be obtained as follows: For the $2m \times 2m$ finite lattice, we denote the configuration of its top and right spins by $s_1 \oplus s_2 \oplus s_3 \oplus s_4$, each s_j representing m-spins. The first guess of the weights can be expressed as

$$\Lambda_{s_1 \oplus s_2 \oplus s_3 \oplus s_4} = \Lambda^S_{s_1} \times \Lambda^S_{s_2} \times \Lambda^S_{s_3} \times \Lambda^S_{s_4},$$

where the $\Lambda^S_{s_i}$ are given by the partition function of an $m \times m$ lattice conditioned on one edge (see Eq. (3.1)). Using the weights we can compute the particular factored solution for the $2m \times 2m$ lattice with spin bath. From this computation an improved guess for the weights can be obtained as follows.

We assume that the $4m$ spins $s_1 \oplus s_2 \oplus s_3 \oplus s_4$ are grouped into $2m$ pairs. If for any configuration of these spins there is a pair in which two adjacent spins are misaligned, then the improved weigth $\Lambda_{s_1 \oplus s_2 \oplus s_3 \oplus s_4} = 0$. For the other configurations, in each pair the two spins have the same value, and thus, they can be represented by one "block spin". There are $2m$ block spins totally, and we denote them by $\tilde{s}_1 \oplus \tilde{s}_2$. Correspondingly, the weights $\Lambda_{s_1 \oplus s_2 \oplus s_3 \oplus s_4}$ can be written as $\Lambda_{\tilde{s}_1 \oplus \tilde{s}_2}$. Note that during the computation of the particular factored solution for the $2m \times 2m$ lattice with spin bath, the partition function of the sublattice shown in Fig. 1 conditioned on $s_5 \oplus s_6$ can be obtained. Let

$$\Lambda_{\tilde{s}_1 \oplus \tilde{s}_2} = \Lambda_{s_5 \oplus s_6};$$

thus, a new set of weights is obtained, by which the iterative process can be repeated until the approximations to Z converge. The above method can be considered as a reverse Kadanoff scaling.

In [II, 8] some values of ϕ, U, and C computed by the scaling method for a 4×4 Ising model are displayed. The convergence to the thermodynamic limit has not been proved.

In this paper we use the scaling method to compute the Ising model with various sizes. The numerical test shows that the iterative process converges and the results are satisfied, which will be discussed in the next section. Here, we focus attention on the further acceleration of the factored solution by column.

From the preceding section we know that after the corresponding factored operation some boundary effects remain in the factored solution by column. Now we inspect this point more precisely.

In Fig. 2a, where the factored solution by column is sketched, $A\cup B$ is an $m\times(n+1)$ lattice and A is an $m\times n$ lattice. If we denote the free energy per spin for lattice $A\cup B$ by $\phi_{m\times(n+1)}$, then the free energy of the whole lattice is $m(n+1)\,\phi_{m\times(n+1)}$. Similarly, for the lattice A the corresponding quantity is $mn\phi_{m\times n}$. When the factored operation is performed, the difference $m(n+1)\,\phi_{m\times(n+1)}-mn\phi_{m\times n}$ is computed. We study it in detail. Because $m(n+1)-mn=m$, in the difference there should be a term which approximates m-spin free energy. This term can be expressed approximately as $m\phi$, where ϕ, as before, is the free energy per spin in the thermodynamic limit. Moreover, some boundary effects are included in the difference. For the lattice $A\cup B$ and sub-lattice A shown in Fig. 2a, the vertical boundaries have the same length, but in the horizontal direction the boundary of $A\cup B$ is one unit longer than the boundary of A. If we note that there are two horizontal boundaries, up and down, and recall that the boundary effect per unit length is denoted by f in Section 2, then there should be a term $2f$ in the difference. In summary, if we denote the difference by $m\phi_{m,n+1}$, we have

$$\begin{aligned} m\phi_{m,n+1} &= m(n+1)\,\phi_{m\times(n+1)}-mn\phi_{m\times n} \\ &= \log\frac{Z_{m\times(n+1)}}{Z_{m\times n}} \\ &= m\phi+2f+o(1), \end{aligned} \tag{5.1}$$

where $o(1)$ denotes the error due to the other finite-size effects and goes to zero as m, n tend to infinity. As compared with (4.4) it is clear that the $\phi_{m,n+1}$ defined by (5.1) is just the factored solution by column. And we know that the term $2f$ in (5.1) reduces the accuracy of $\phi_{m,n+1}$ as an approximation to ϕ. However, the term can be eliminated easily. Besides $\phi_{m,n+1}$ we compute $\phi_{m-1,n}$, according to (5.1),

$$(m-1)\,\phi_{m-1,n}=(m-1)\,\phi+2f+o(1). \tag{5.2}$$

Subtracting (5.2) from (5.1), we have

$$\begin{aligned} \bar{\phi}_{m,n+1} &= m\phi_{m,n+1}-(m-1)\,\phi_{m-1,n} \\ &= \phi+o(1). \end{aligned} \tag{5.3}$$

$\tilde{\phi}_{m,n+1}$ is a better approximation to ϕ than the factored solution by column $\phi_{m,n+1}$. Similar approximations to the bulk internal energy U and the bulk specific heat C can be derived in the same way and are denoted by $\tilde{U}$ and $\tilde{C}$, respec-

Here, it should be pointed out that to eliminate the term $2f$ from (5.1) we can use any $\phi_{p,q}$; the only requirement is $p \neq m$. We chose $\phi_{m-1,n}$ for convenience of programming. In the pratical computation we take $n = m$.

In the following the expression (5.3) is explained in a different way. If the $m \times n$ Ising model is wrapped on a torus and in the thermodynamic limit n is allowed to approach infinity before m, following Thompson [I, 6], we have

$$\begin{aligned}\phi &= \lim_{m\to\infty} m^{-1} \log \lambda_1 = \frac{1}{2}\log(2\sinh(2\beta)) \\ &\quad + \lim_{m\to\infty} (2m)^{-1} \sum_{k=0}^{k=m-1} \gamma_{2k+1} \\ &= \frac{1}{2}\log(2\sinh(2\beta)) + (2\pi)^{-1} \int_0^{\pi} \cosh^{-1}((\cosh(2\beta)\coth(2\beta) - \cos(\theta))\, d\theta, \qquad (5.4)\end{aligned}$$

where λ_1 is the maximum eigenvalue of the corresponding 2^m by 2^m transfer matrix and γ_k is defined by $\cosh(\gamma_k) = \cosh(2\beta)\coth(2\beta) - \cos(\pi k/m)$. From (5.4) we know that using $m^{-1}\log\lambda_1$ instead of ϕ corresponds to using the summation $(2m)^{-1}\sum_{k=0}^{k=m-1}\gamma_{2k+1}$ instead of the integral. From the point of view of numerical analysis this means that the integral is calculated by the rectangle rule formula, and the number of intervals is proportional to m. On the other hand we know from (4.4) that the factored solution by column $\phi_{m,n+1}$ is an approximation to $m^{-1}\log\lambda_1$. Thus we see that the algorithm expressed by (5.3) can be considered as the Richarson extrapolation method in numerical analysis, which improves the accuracy of the approximate integral calculation. From now on (5.3) is called the extra linear extrapolation algorithm.

From (5.1) and (5.2) we can also derive a formula to compute the boundary free energy f. However, we should make a further assumption on the term $o(1)$ appearing in (5.1). Denoting the term by $\psi(m, m+1)$, we asume not only $\psi(m, n+1) \to 0$ as $m, n \to \infty$, but also

$$m\psi(m-1, n) - (m-1)\,\psi(m, n+1) \to 0, \qquad \text{as} \quad m, n \to \infty. \qquad (5.5)$$

This assumption means that either the term $o(1)$ has a higher order than m^{-1} or its main part can be expressed as $Am^{-\alpha}$, $0 < \alpha \leqq 1$, and the coefficient A is independent of m. In fact, it seems reasonable to consider the term $o(1)$ very close to the difference between the free energy computed for a finite lattice with periodic conditions and the corresponding thermodynamic limit. If it is true, then this term will decay exponentially with m. At the end of this section the validity of this assumption is discussed by considering the high-temperature expansion for the

boundary free energy f. Mainly it is justified by the numerical results which are derived from this assumption and is presented in the next section.

Under assumption (5.5), multiplying (5.2) by m, and subtracting the result from $(m-1)\times(4.1)$, we have

$$f_{m,n+1} \equiv 2^{-1}m(m-1)(\phi_{m-1,n}-\phi_{m,n+1}) = f + o(1); \tag{5.6}$$

$f_{m,n+1}$ can be taken as an approximation to the boundary free energy per unit length.

It is clear that similar expressions hold for the approximation to the boundary internal energy and the approximation to the boundary specific heat. They are denoted by $e_{m,n+1}$, $C^b_{m,n+1}$, respectively.

From (5.6) an expression for the boundary free energy f of the Ising model with free boundary conditions can be derived. The expression (5.6) can be written as

$$\lim_{m,n\to\infty} 2^{-1}m(m-1)(\phi_{m-1,n}-\phi_{m,n+1}) = f. \tag{5.7}$$

In (5.7) we allow n go to infinity before m. Then

$$\lim_{m\to\infty} 2^{-1}m(m-1)(\phi_{m-1}-\phi_m) = f, \tag{5.8}$$

where

$$\phi_m = \lim_{n\to\infty} \phi_{m,n+1} = \frac{1}{m}\log\lambda_1, \tag{5.9}$$

which can be obtained from (4.4), and λ_1 is the maximum eigenvalue of the 2^m by 2^m matrix L given by (3.8). Here, to indicate the dependence of λ_1 on m, we denote it by $\lambda_1(m)$. Thus the expression (5.8) can be written as

$$f = \lim_{m\to\infty} \frac{1}{2}\log\left(\frac{\lambda_1^m(m-1)}{\lambda_1^{m-1}(m)}\right). \tag{5.10}$$

Expression (5.10) exhibits the relation between the eigenvalue of the transfer matrix and the boundary thermodynamic functions.

Now we briefly discuss the validity of assumption (5.5). In order to show that assumption (5.5) is reasonable, we compare the f defined by (2.10) with expression (5.7), which is derived on the basis of (5.5). However, it is difficult to do this analytically. Instead, we adopt an alternative way; i.e., we compare the two high-temperature expansions for f which are derived from (2.10) and (5.7) separately, and consider only the first few terms.

It is well known that at high temperature the free energy ϕ can be expanded as a series in $\omega = \tanh(z)$ and the expansion coefficients can be calculated by a com-

binatorial approach (see [I, 5]). If we consider only the first few terms of the series, the corresponding coefficients can be obtained easily and ϕ can be written as

$$\phi = \log 2 + 2 \log \cosh(\beta) + \omega^4 + 2\omega^6 + \tfrac{9}{2}\omega^8 + o(\omega^{10}). \tag{5.11}$$

For the free energy of an $m \times n$ Ising model with free edges, the corresponding expansion is

$$\begin{aligned}\phi_{m\times n} = \log 2 &+ \left(2 - \left(\frac{1}{m} + \frac{1}{n}\right)\right) \log \cosh(\beta) + \left(\frac{1}{m} - 1\right)\left(\frac{1}{n} - 1\right) \omega^4 \\ &+ \left(2 - 3\left(\frac{1}{m} + \frac{1}{n}\right) + \frac{4}{mn}\right) \omega^6 + \left(\frac{9}{2} - \frac{21}{2}\left(\frac{1}{m} + \frac{1}{n}\right)\right. \\ &\left. + \frac{43}{2}\frac{1}{mn}\right) \omega^8 + o(\omega^{10}).\end{aligned} \tag{5.12}$$

In (5.12) let n go to infinity. We have

$$\begin{aligned}\phi_m = \log 2 &+ \left(2 - \frac{1}{m}\right) \log \cosh(\beta) + \left(1 - \frac{1}{m}\right) \omega^4 + \left(2 - \frac{3}{m}\right) \omega^6 \\ &+ \left(\frac{9}{2} - \frac{21}{2m}\right) \omega^8 + o(\omega^{10}).\end{aligned} \tag{5.13}$$

Substituting (5.11) and (5.13) into (2.10), or substituting (5.12) into (5.7), we obtain the same expansion:

$$f = -2^{-1}\left(\log \cosh(\beta) - \omega^4 + 3\omega^6 + \frac{21}{2}\omega^8\right) + o(\omega^{10}). \tag{5.14}$$

To some extent this result shows us that assumption (5.5) is reasonable. Here we have considered only the coefficients of the terms to ω^9 because when the power increases the computation of the corresponding coefficient becomes very complicated.

6. Numerical Results and Discussion

In this section we present and discuss some numerical results. First, the approximate bulk thermodynamic functions computed by the various factored solutions as well as the two further acceleration methods, i.e., the scaling and the extra linear extrapolation algorithm, are given. From these results the different methods can be compared. Furthermore, the boundary thermodynamic functions computed by the extra linear extrapolation algorithm from which the algorithm is tested, are displayed. Finally, we estimate the critical point by combining the different numerical results with the finite-size-scaling theory.

For the bulk thermodynamic functions, our results can be compared with [II, 14], in which the $N \times N$ Ising model with free edges has been computed by the Monte Carlo method for $N \leqq 100$. Our methods, i.e., the particular factored solution, the scaling, and the extra linear extrapolation, have shown much faster convergence than the Monte Carlo. For the boundary thermodynamic functions of the Ising model our numerical results are apparently the first and their convergence looks good. The approximate boundary free energy, internal energy, and specific heat are consistent with the theoretical predictions and reveal the specific features of the thermodynamic functions. Our estimate for the critical point is also better than that of the Monte Carlo method and comparable with the numerical renormalization group results in e.g., [I, 5; II, 15].

In Tables Ia–Ic we display $\phi_{m,n+1}$, $U_{m,m+1}$, and $C_{m,m+1}$ computed by the factored solution by column for $m = 4, 8, 12$ and some β. For the sake of comparision the corresponding values for an $8 \times \infty$ lattice as well as the exact values of ϕ, U, and C are also given. In Tables IIa–IIc and IIIa–IIIc we display $\phi_{m \times m}$, $U_{m \times m}$, and $C_{m \times m}$ computed by the general ($l = 7$) and particular factored solution for the same m and β, respectively. In Tables IVa–IVc and Va–Vc the same thermodynamic functions computed by the scaling method and the extra linear extrapolation algorithm are displayed. For the scaling method the lattices are $m \times m$. For the extra linear extrapolation, according to formula (5.3) and similar formulas, the relevant maximum lattice size is $m \times (m+1)$. However, the computational labor required by the scaling is still much greater than the latter because it is an iterative algorithm and uses spin bath.

Looking at these tables we can come to the following conclusions:

(1) Except for the specific heat for temperatures near or below criticality, our numerical approximation to any thermodynamic function converges reasonably well to the corresponding thermodynamic limit as the lattice sizes increase. The convergence is most rapid for the free energy, less rapid for the internal energy and specific heat.

(2) The results computed by the factored solution by column for a finite lattice are almost the same as those for an infinitely long Ising strip. It means that the factored operation accelerates the convergence to the thermodynamic limit.

(3) When we compare the results in Table I with those in Tables II and III, we know that the factored solution by column has the lowest accuracy and the particular factored solution gives the most satisfying results. This result supports our preceding discussions.

(4) From Tables IV and V, we find that the solutions of the scaling method and the extra linear extrapolation algorithm are more accurate than the particular factored solutions. The scaling and the extra linear extrapolation algorithm are comparable in accuracy.

In Tables Ic, IIc, IIIc, IVc, and Vc, near criticality the approximate specific heats do not converge seriously. The reason is that the lattice sizes calculated by us are

TABLE I

a. Convergence of factored solution by column to the free energy ϕ

β	$\phi_{4,5}$	$\phi_{8,9}$	$\phi_{12,13}$	$\phi_{8\times\infty}$	ϕ(exact)
0.1	0.7020	0.7026	0.7028	0.7026	0.7032
0.2	0.7291	0.7318	0.7327	0.7318	0.7345
0.3	0.7770	0.7838	0.7860	0.7838	0.7906
0.4	0.8496	0.8645	0.8694	0.8645	0.8794
0.45	0.8967	0.9188	0.9266	0.9189	0.9436
0.5	0.9515	0.9843	0.9968	0.9845	1.026
0.6	1.083	1.143	1.166	1.144	1.210
0.7	1.237	1.321	1.349	1.321	1.404
0.8	1.404	1.504	1.537	1.504	1.602
0.9	1.576	1.689	1.720	1.689	1.801
1.0	1.750	1.876	1.917	1.876	2.001

b. Convergence of factored solution by column to the internal energy U

β	$U_{4,5}$	$U_{8,9}$	$U_{12,13}$	$U_{8\times\infty}$	U(exact)
0.1	0.1774	0.1904	0.1947	0.1904	0.2034
0.2	0.3699	0.3991	0.4088	0.3991	0.4282
0.3	0.5944	0.6495	0.6679	0.6495	0.7045
0.4	0.8664	0.9826	1.023	0.9831	1.106
0.45	1.019	1.196	1.271	1.199	1.513
0.5	1.174	1.421	1.533	1.419	1.746
0.6	1.446	1.717	1.796	1.720	1.909
0.7	1.620	1.812	1.862	1.810	1.964
0.8	1.702	1.846	1.891	1.846	1.985
0.9	1.734	1.861	1.905	1.861	1.993
1.0	1.745	1.868	1.911	1.868	1.997

c. Convergence of factored solution by column to the specific heat C

β	$C_{4,5}$	$C_{8,9}$	$C_{12,14}$	$C_{8\times\infty}$	C(exact)
0.1	0.0182	0.0196	0.0201	0.0196	0.0210
0.2	0.0822	0.0899	0.0925	0.0899	0.0977
0.3	0.2219	0.2543	0.2650	0.2543	0.2863
0.4	0.4742	0.6312	0.7021	0.6353	0.8626
0.45	0.6285	0.9163	1.100	0.9294	1.605
0.5	0.7627	1.066	1.140	1.002	0.7240
0.6	0.8215	0.5928	0.4307	0.5546	0.3134
0.7	0.5951	0.2535	0.2213	0.2584	0.1581
0.8	0.3240	0.1380	0.1233	0.1474	0.0830
0.9	0.1480	0.0808	0.0698	0.0877	0.0441
1.0	0.0604	0.0477	0.0399	0.0444	0.0234

TABLE II

a. Convergence of general factored solution ($l=7$) to the free energy ϕ

β	4×4 array	8×8 array	12×12 array	ϕ(exact)
0.1	0.7032	0.7032	0.7032	0.7032
0.2	0.7345	0.7345	0.7345	0.7345
0.3	0.7901	0.7905	0.7905	0.7906
0.4	0.8754	0.8785	0.8790	0.8794
0.45	0.9310	0.9383	0.9404	0.9436
0.5	0.9960	1.011	1.016	1.026
0.6	1.153	1.188	1.200	1.210
0.7	1.337	1.387	1.398	1.404
0.8	1.537	1.590	1.598	1.602
0.9	1.744	1.792	1.798	1.801
1.0	1.953	1.995	1.999	2.001

b. Convergence of general factored solution ($l=7$) to the internal energy U

β	4×4 array	8×8 array	12×12 array	U(exact)
0.1	0.2034	0.2034	0.2034	0.2034
0.2	0.4274	0.4282	0.4282	0.4282
0.3	0.6943	0.7032	0.7042	0.7045
0.4	1.022	1.079	1.094	1.106
0.45	1.205	1.320	1.369	1.513
0.5	1.392	1.576	1.663	1.746
0.7	1.942	2.019	1.994	1.964
0.8	2.047	2.031	2.004	1.985
0.9	2.082	2.026	2.005	1.993
1.0	2.086	2.020	2.004	1.997

c. Convergence of general factored solution ($l=7$) to the specific heat C

β	4×4 array	8×8 array	12×12 array	C(exact)
0.1	0.0210	0.0210	0.0210	0.0210
0.2	0.0967	0.0976	0.0976	0.0977
0.3	0.2662	0.2828	0.2853	0.2863
0.4	0.5714	0.7166	0.7806	0.8626
0.45	0.7567	1.038	1.223	1.605
0.5	0.9201	1.221	1.303	0.7249
0.6	1.015	0.6915	0.3767	0.3134
0.7	0.7617	0.1674	0.0941	0.1581
0.8	0.3994	−.0053	0.0214	0.0830
0.9	0.1187	−.0543	−.0030	0.0441
1.0	−.0049	−.0645	−.0106	0.0234

TABLE III

a. Convergence of particular factored solution to the free energy ϕ

β	4×4 array	8×8 array	12×12 array	ϕ(exact)
0.1	0.7032	0.7032	0.7032	0.7032
0.2	0.7345	0.7345	0.7345	0.7345
0.3	0.7904	0.7905	0.7906	0.7906
0.4	0.8769	0.8789	0.8792	0.8794
0.45	0.9339	0.9396	0.9411	0.9436
0.5	1.001	1.014	1.019	1.026
0.6	1.163	1.196	1.205	1.210
0.7	1.355	1.396	1.402	1.404
0.8	1.560	1.579	1.601	1.602
0.9	1.769	1.798	1.800	1.801
1.0	1.979	1.999	2.000	2.001

b. Convergence of particular factored solution to the internal energy U

β	4×4 array	8×8 array	12×12 array	U(exact)
0.1	0.2034	0.2034	0.2034	0.2034
0.2	0.4280	0.4282	0.4282	0.4282
0.3	0.6997	0.7041	0.7044	0.7045
0.4	1.043	1.089	1.099	1.106
0.45	1.239	1.345	1.389	1.513
0.5	1.440	1.617	1.699	1.746
0.6	1.792	1.957	1.949	1.909
0.7	2.004	2.017	1.980	1.964
0.8	2.085	2.014	1.992	1.985
0.9	2.094	2.008	1.997	1.993
1.0	2.078	2.005	1.999	1.997

c. Convergence of particular factored solution to the specific heat C

β	4×4 array	8×8 array	12×12 array	C(exact)
0.1	0.0210	0.0210	0.0210	0.0210
0.2	0.0974	0.0976	0.0977	0.0977
0.3	0.2743	0.2851	0.2860	0.2863
0.4	0.6082	0.7498	0.8070	0.8626
0.45	0.8139	1.108	1.302	1.605
0.5	0.9901	1.288	1.330	0.7249
0.6	1.043	0.5614	0.2388	0.3134
0.7	0.6727	0.0347	0.0781	0.1581
0.8	0.2236	−.0443	0.0503	0.0830
0.9	−.0700	−.0352	0.0282	0.0441
1.0	−.2002	−.0231	0.0134	0.0234

TABLE IV

a. Convergence of scaling method to the free energy ϕ

β	4×4 array	8×8 array	12×12 array	ϕ(exact)
0.1	0.7032	0.7032	0.7032	0.7032
0.2	0.7345	0.7345	0.7345	0.7345
0.3	0.7908	0.7906	0.7906	0.7906
0.4	0.8808	0.8795	0.8794	0.8794
0.45	0.9433	0.9424	0.9426	0.9436
0.5	1.019	1.021	1.023	1.026
0.6	1.197	1.205	1.208	1.210
0.7	1.392	1.400	1.402	1.404
0.8	1.593	1.599	1.601	1.602
0.9	1.794	1.799	1.800	1.801
1.0	1.996	1.999	2.000	2.001

b. Convergence of scaling method to the internal energy U

β	4×4 array	8×8 array	12×12 array	U(exact)
0.1	0.2034	0.2034	0.2034	0.2034
0.2	0.4285	0.4282	0.4282	0.4282
0.3	0.7098	0.7045	0.7044	0.7045
0.4	1.121	1.110	1.107	1.106
0.45	1.381	1.418	1.441	1.513
0.5	1.621	1.700	1.731	1.746
0.6	1.900	1.923	1.919	1.909
0.7	1.990	1.979	1.971	1.964
0.8	2.013	1.995	1.990	1.985
0.9	2.016	2.000	1.997	1.993
1.0	2.014	2.002	1.999	1.997

c. Convergence of scaling method to the specific heat C

β	4×4 array	8×8 array	12×12 array	C(exact)
0.1	0.0210	0.0210	0.0210	0.0210
0.2	0.0981	0.0976	0.0977	0.0977
0.3	0.2970	0.2865	0.2860	0.2863
0.4	0.7974	0.8612	0.8692	0.8620
0.45	1.057	1.327	1.504	1.605
0.5	1.056	1 074	0.9560	0.7249
0.6	0.5642	0.3539	0.3096	0.3134
0.7	0.2153	0.1378	0.1435	0.1581
0.8	0.0572	0.0572	0.0703	0.0830
0.9	−.0090	0.0212	0.0255	0.0441
1.0	−.0335	0.0450	0.0149	0.0234

TABLE V

a. Convergence of linear extrapolation algorithm to the free energy ϕ

β	$\tilde{\phi}_{4,5}$	$\tilde{\phi}_{8,9}$	$\tilde{\phi}_{12,13}$	ϕ(exact)
0.1	0.7032	0.7032	0.7032	0.7032
0.2	0.7345	0.7345	0.7345	0.7345
0.3	0.7906	0.7906	0.7906	0.7906
0.4	0.8791	0.8793	0.8794	0.8794
0.45	0.9389	0.9416	0.9423	0.9436
0.5	1.010	1.020	1.024	1.026
0.6	1.187	1.209	1.210	1.210
0.7	1.391	1.405	1.404	1.404
0.8	1.602	1.602	1.602	1.602
0.9	1.809	1.801	1.801	1.801
1.0	2.012	2.000	2.000	2.001

b. Convergence of linear extrapolation algorithm to the internal energy U

β	$\tilde{U}_{4,4}$	$\tilde{U}_{8,9}$	$\tilde{U}_{12,13}$	U(exact)
0.1	0.2034	0.2034	0.2034	0.2034
0.2	0.4284	0.4282	0.4282	0.4282
0.3	0.7062	0.7045	0.7045	0.7045
0.4	1.083	1.103	1.106	1.106
0.45	1.312	1.398	1.432	1.513
0.5	1.551	1.717	1.774	1.746
0.6	1.943	1.967	1.912	1.909
0.7	2.106	1.964	1.962	1.964
0.8	2.099	1.980	1.985	1.985
0.9	2.045	1.997	1.993	1.993
1.0	2.005	1.996	1.997	1.997

c. Convergence of linear extrapolation algorithm to the specific heat C

β	$\tilde{C}_{4,5}$	$\tilde{C}_{8,9}$	$\tilde{C}_{12,13}$	C(exact)
0.1	0.0210	0.0210	0.0210	0.0210
0.2	0.0979	0.0977	0.0977	0.0977
0.3	0.2874	0.2864	0.2863	0.2863
0.4	0.6970	0.8213	0.8524	0.8620
0.45	0.9644	1.321	1.548	1.605
0.5	1.173	1.413	1.171	0.7249
0.6	1.026	0.0580	0.1981	0.3134
0.7	0.2680	0.0418	0.1722	0.1581
0.8	−.2966	0.0996	0.0866	0.0830
0.9	−.4129	0.0636	0.0445	0.0441
1.0	−.2950	0.0323	0.0234	0.0234

still not large enough. In principle, the extrapolations included in our algorithms are based on the decomposition of the thermodynamic quantities into the bulk terms plus boundary corrections. Strictly speaking, this decomposition is correct only for the temperature region which is away from the criticality and marked by the rounding temperature T^*. Therefore, if we use the extrapolation at the criticality, the effects are not clear. However, as the lattice sizes increases, the temperature $T^* \to T_c$, we can expect that our extrapolation methods will be effective for more temperatures which are close to T_c.

In Fig. 3 the variation of the approximate bulk specific heat $\tilde{C}_{m\times(m+1)}$ computed by the extra linear extrapolation algorithm with β is shown. Under the condition of finite-size lattice, the logarithmic singularity in the specific heat transforms into a smooth peak. When the lattice size increases, the peak moves to the critical point, at the same time the width of the peak becomes narrow and the height of the peak increases. It suggests that the critical exponents $\alpha = \alpha' = 0_{\log}$. It is also noted that the curve of the approximate specific heat given by the extra linear extrapolation algorithm for fixed m has a small oscillation at $\beta > \beta_c$. When m increases the amplitude of the oscillation is reduced and the position at which the oscillation occurs moves to the critical point. If we carefully observe the particular factored solution, a similar phenomenon can be found. However, for the factored solution the oscillation is mild. Without separating the boundary effect this phenomenon could not be observed.

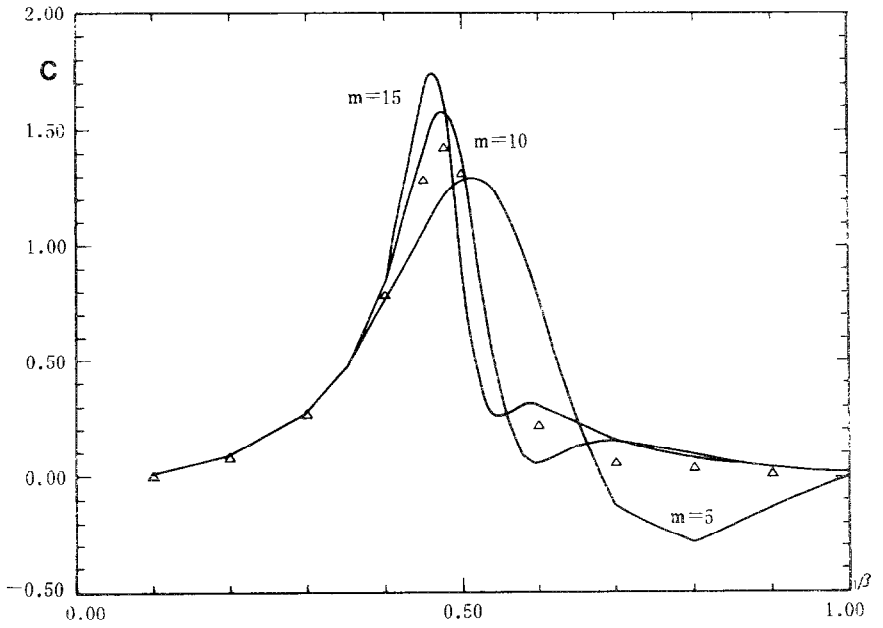

FIG. 3. The bulk specific heat computed with the extra linear extrapolation algorithm. The triangles are the particular factored solution for $m = 12$.

In Figs. 4a, 4b, and 4c, the curves of the approximate boundary free energy $f_{m,m+1}$, the approximate boundary internal energy $e_{m,m+1}$, and the approximate boundary specific heat $c^b_{m,m+1}$ computed by formula (5.6) and similar formulas for $m=5$, 10, and 15 are shown.

An interesting point is that from Fig. 4a, we guess that when the temperature goes to zero, the boundary free energy can be approximated by $-\beta/2$ very well. We also compute the boundary free energy by the series expansion (5.14) for $\beta=0.1$, 0.2, 0.3, and 0.4. The corresponding numerical results are -0.0025, -0.0108, -0.0270, and -0.0562, respectively. They are very close to the results shown in Fig. 4a, which signifies that assumption (5.5) is reasonable and formulas (5.6), (5.10), and (5.14), which express the approximate or exact boundary free energy, are correct.

In Fig. 4b, for the boundary internal energy as for the bulk specific heat, the logarithmic singularity is replaced by a smooth peak. As lattice size increases, the width of the peak becomes narrow and its position moves to the critical point from the low temperature side. In Section 2 it was stated that in the thermodynamic limit, superimposed on the logarithmic infinity, a discontinuity exists in e at β_c. Under the finite-lattice condition this phenomenon is shown in the nonsymmetry of the $e_{m,m+1}$ curves. The interesting point is that although we have calculated only

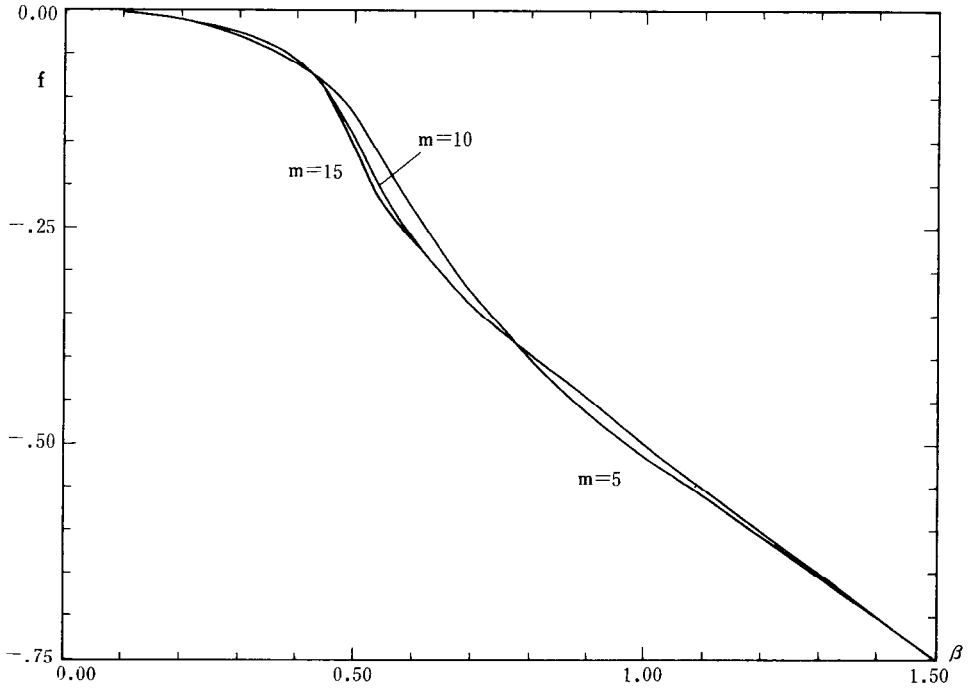

FIG. 4a. The boundary free energy computed with the extra linear extrapolation algorithm.

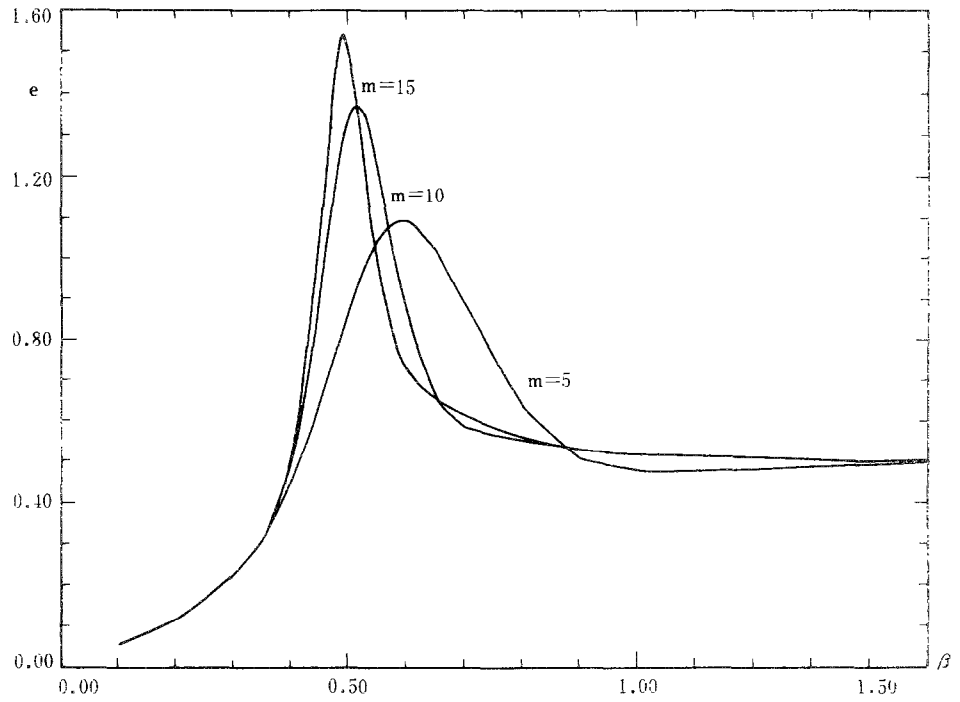

FIG. 4b. The boundary internal energy computed with the extra linear extrapolation algorithm.

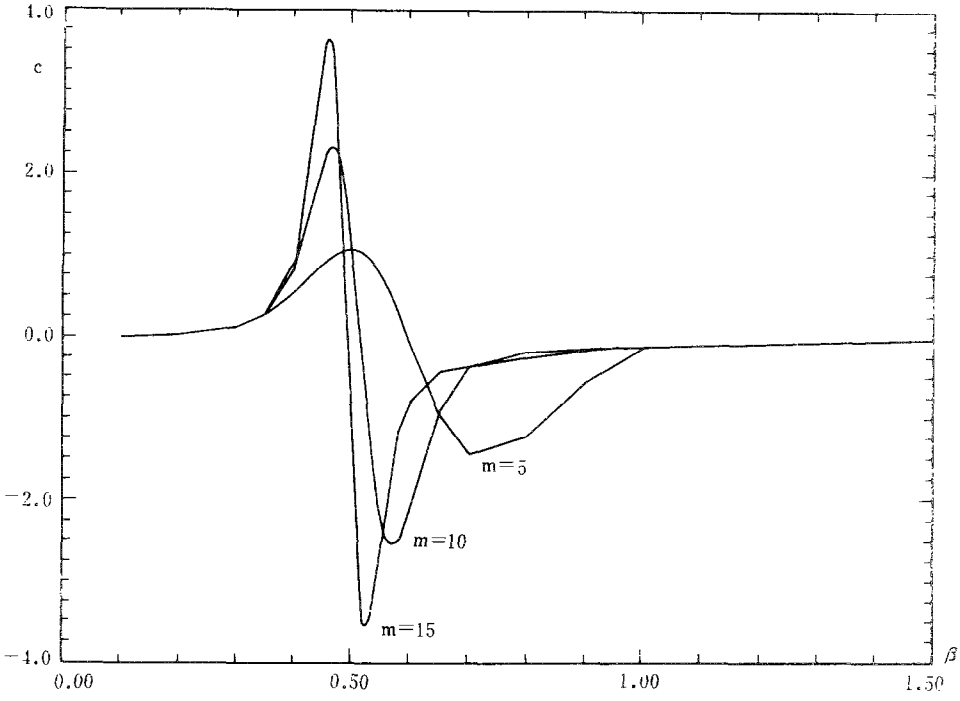

FIG. 4c. The boundary specific heat computed with the extra linear extrapolation algorithm.

relatively small lattices, at the two ends of these $e_{m,m+1}$ curves the computed values appear to converge already. If the values at the two ends, for example, at $\beta = 0.1$ and $\beta = 2.5$, are compared, it is found that for each m the difference is almost exactly 0.5, i.e., the jump which occurs at β_c in the thermodynamic limit.

In Fig. 4c for every m the two ends of the $c^b_{m,m+1}$ curve approach the x-axis from the positive and the negative direction, respectively. In the middle of the curve a positive maximum continuously but rapidly transforms into a negative minimum. This graph corresponds to the singularity t^{-1} in the thermodynamic limit. As m increases both the maximum and the minimum move to the critical point from the low temperature side, and at the same time the distance between them decreases; however, the amplitude increases. It is predictable that the position of either the maximum or the minimum will coincide with β_c in the thermodynamic limit and the amplitude will go to infinity at the same time.

Next, we estimate the critical point. From the numerical computation we know that the approximate bulk specific heat obtained by any method mentioned for each finite lattice has a maximum which occurs at a certain temperature. This temperature can be considered as an m-dependent pseudo-critical point. Similarly, for the boundary thermodynamic functions we can also define the pseudo-critical point. For the boundary internal energy the pseudo-critical point is the temperature at which for a certain finite lattice the approximate boundary internal energy achieves its maximum value. For the approximate boundary specific heat, two different pseudo-critical points can be defined—one is the temperature at which the boundary specific heat achieves its maximum; the other is that at which the minimum boundary specific heat occurs.

The real critical temperature can be estimated as follows. For each group of data which is given by one method for one thermodynamic function, we assume that the pseudo-critical point is a linear function of m^{-1}, i. e., $\beta_{\max(\min)} = a_0 + a_1 m^{-1}$. Then, a_0 and a_1 can be estimated by the least-squares method. It is clear that the value of a_0 can be considered as an estimate of the real critical point and this estimate depends not only on the type of pseudo-critical point but also on the lattice sizes used in the least-squares computation.

In Table VIa the approximate critical points estimated from the maximum bulk specific heat are given. The data in different rows correspond to different methods which have been used to compute the bulk specific heat. In Table VIb the approximate critical points estimate from different boundary thermodynamic quantities are shown.

We recall that the exact critical point value is 0.440685.... From Table VIa, we know that the scaling method gives the best estimate and for the particular factored solution the estimate has the lowest accuracy. For the scaling method if we use the pseudo-critical points with linear dimensions $m = 8, 10$ in the least-squares computation the approximate critical point is 0.4415. The relative error is less than 0.002. However, it should be pointed out that the scaling method requires more computational labor than the other methods, which restrains us from computation of larger lattices on our computer VAX.780. Thus we cannot obtain a more exact

TABLE VI

a. The critical point estimated from maximum bulk specific heat values

Numerical method	Lattice size	Approximate critical point	Lattice size	Approximate critical point	Lattice size	Approximate critical point
Factored solution	$m = 4, 6, 8, 10$	0.4346	$m = 6, 8, 10$	0.4373	$m = 8, 10$	0.4380
Scaling method	$m = 4, 6, 8, 10$	0.4435	$m = 6, 8, 10$	0.4420	$m = 8, 10$	0.4415
Extra linear extrapolation	$m = 4, 6, 8, 10$	0.4377	$m = 6, 8, 10$	0.4391	$m = 8, 10$	0.4395

b. The critical point estimated from boundary thermodynamic function computed by extra linear extrapolation algorithm

Type of pseudo-critical point	Lattice size	Approximate critical point	Lattice size	Approximate critical point	Lattice size	Approximate critical point
Maximum internal energy	$m = 11, 12, 13, 14, 15$	0.4434	$m = 13, 14, 15$	0.4432	$m = 14, 15$	0.4430
Maximum specific heat	$m = 11, 12, 13, 14, 15$	0.4406	$m = 13, 14, 15$	0.4407	$m = 14, 15$	0.4407
Minimum specific heat	$m = 11, 12, 13, 14, 15$	0.4388	$m = 13, 14, 15$	0.4393	$m = 14, 15$	0.4395

estimate from the scaling. If for the extra linear extrapolation algorithm we use the pseudo-critical points for $m = 14, 15$, we obtain the approximate critical point 0.4403, whose relative error is less than 0.001. From Table VIb we know that the estimate computed from the maximum boundary specific heat has the highest accuracy. If in the least-squares method $m = 13, 14, 15$ are considered, the exact result is given in four significant digits. In the last column of Table VIb the maximum relative error is only 0.005.

The above results can be compared with those obtained by other numerical methods. In [I, 5], the approximate critical point computed by the cumulant expansion method was given. The value is 0.4302 and has the relative error 0.011. In [II, 14], the $N \times N$ Ising model for $N \leqq 100$ was computed by the Monte Carlo method, and the autor declared that the estimate for the critical point is correct to better then 0.005. It can be compared with the maximum error in the last column in Table VIb. In [II, 15], Nightingale obtained some critical point estimates which are slightly better than ours, but it should be pointed out that in [II. 15] the critical point was estimated by means of the analytic expression of the inverse correlation length of an $n \times \infty$ Ising strip. Thus, it is not a "purely" numerical result.

Finally, we briefly review the particular factored solution, the scaling method, and the extra linear extrapolation algorithm.

The particular factored solution almost eliminates the finite-size effect due to the "dangling bonds." It is a satisfying member in the factored solution family and accelerates the convergence of finite-lattice quantities to the thermodynamic limit. Although its accuracy is lower than that of the scaling and the extra linear extrapolation algorithms, the method is very simple and desirable.

The scaling method gives high accuracy, especially when the lattice size is small. With the lattice size increasing, the thermodynamic functions computed by the scaling converge to their thermodynamic limits. From computational results the critical point can be estimated better. However, this method requires more computational time and storage space, which restricts its use. If we could combine this method with Monte Carlo, it might produce a more efficient and flexible method. Ideas somewhat similar to this approach have been considered by Goodman and Sokal [II, 11].

The extra linear extrapolation algorithm also gives high accuracy and does not need much increase of computational labor. In addition, this algorithm can be used to compute the boundary thermodynamic functions and give satisfactory results. In further work we shall study how the boundary magnetic quantities for a lattice model can be computed with a similar algorithm and try to combine the extra linear extrapolation algorithm with other methods.

ACKNOWLEDGMENTS

I am grateful to Professor Alexandre J. Chorin for his kind support and for many helpful discussions and comments. I also extend thanks to Dr. C. C. Chang for his useful comments on my paper. This work was carried out while the author was visiting the Department of Mathematics, University of California, Berkeley, and the Lawrence Berkeley Laboratory and was supported in part by the Applied Mathematics subprogram of the Office of Energy Research, U.S. Department of Energy, under Contract BE-AC03-76SF00098. It was also supported in part by the National Natural Science Foundation of China.

REFERENCES

I. *Books*

1. M. N. BARBER, "Finite-Size Scaling," in *Phase Transitions and Critical Phenomena*, Vol. 8, edited by C. Domb and J. L. Lebowits (Academic Press, New York/London, 1983), p. 145.
2. K. S. BINDER, *Monte Carlo Methods in Statistical Physics* (Springer-Verlag, Berlin, 1979).
3. K. S. BINDER, "Critical Behaviour at Surfaces," in *Phase Transitions and Critical Phenomena*, Vol. 8, edited by C. Domb and J. L. Lebowits (Academic Press, New York/London, 1983), p. 1.
4. R. B. ISRAEL, *Convexity in the Theory of Lattice Gases* (Princeton Univ. Press, Princeton, NJ, 1979), Chap. 1.
5. T. NIEMIEJER AND J. M. J. LEEUWEN, "Renormalization Theory for Ising-like Spin Systems," in *Phase Transitions and Critical Phenomena*, Vol. 6, edited by C. Domb and M. S. Green (Academic Press, New York, 1976), p. 425.
6. C. J. THOMPSON, *Mathematical Statistical Mechanics* (Princeton Univ. Press, Princeton, NJ, 1972), p. 127.
7. P. G. WATSON, "Surface and Size Effects in Lattice Models," in *Phase Transitions and Critical Phenomena*, Vol. 2, edited by C. Domb and M. S. Green (Academic Press, New York/London, 1972), p. 101.

II. *Journals*

1. H. Au-Yang, *J. Math. Phys.* **14**, 937 (1973).
2. H. Au-Yang and M. E. Fisher, *Phys. Rev. B* **11**, 3469 (1975).
3. H. Au-Yang and M. E. Fisher, *Phys. Rev. B* **21**, 3965 (1980).
4. M. N. Barber, I. Peschel, and P. A. Pearce, *J. Stat. Phys.* **37**, 497 (1984).
5. K. S. Binder and P. C. Hohenberg, *Phys. Rev. B* **9**, 2194 (1974).
6. K. S. Binder, *J. Comput. Phys.* **59**, 1 (1985).
7. H. W. J. Blote and M. P. Nightingale, *Physica. A.* **112**. 405 (1982).
8. A. J. Chorin, *Commun. Math. Phys.* **99**, 501 (1985).
9. M. E. Fisher and A. E. Ferdinand, *Phys. Rev. Lett.* **19**, 169 (1967).
10. A. E. Ferdinand and M. E. Fisher, *Phys. Rev.* **185**. 832 (1969).
11. J. Goodman and A. D. Sokal, *Phys. Rev. Lett.* **56**, 1015 (1986).
12. C. J. Hamer and M. N. Barber, *J. Phys. A* **14**. 2009 (1981).
13. D. P. Landau, *Phys. Lett. A* **47**, 41 (1974).
14. D. P. Landau, *Phys. Rev. B* **9**, 2194 (1976).
15. P. Nightingale, *Physica A* **83**, 561 (1976).
16. P. Nightingale, *J. Appl. Phys.* **53** (11), 7927 (1982).